Supporting Information for

Metal-Center Exchange of Tetrahedral Cages: Single Crystal to Single Crystal and Spin Crossover Properties

*Feng-Li Zhang[a], Jia-Qian Chen[a], Long-Fang Qin[a], Lei Tian[a], Zaijun Li[a], Xuehong Ren[b], Zhi-Guo Gu[a]**

[a] *The Key Laboratory of Food Colloids and Biotechnology, Ministry of Education, School of Chemical and Material Engineering, Jiangnan University, Wuxi 214122, P.R. China*
[b] *The Key Laboratory of Eco-textiles of Ministry of Education, College of Textiles and Clothing, Jiangnan University, Wuxi 214122, P.R. China*

E-mail: zhiguogu@jiangnan.edu.cn

Table of contents

1. Experimental Section

All reagents and solvents were reagent grade, purchased from commercial sources and used without further purification. Infrared spectra were measured on an ABB Bomem FTLA 2000-104 spectrometer with KBr pellets in the 500-4000 cm^{-1} region. NMR spectra were recorded on AVANCE III (400 MHz) instrument at 298 K using standard Varian or Bruker software, and chemical shifts were reported in parts per milion (ppm) downfield from tetramethylsilane. Element analyses were conducted on elementar corporation vario EL III analyzer. UV/vis absorbance spectra were collected on Shimadzu UV-2101 PC scanning spectrophotometer. The TG curves were carried out by using TGA/1100SF thermo grabinetric analyzer with a temperature range of 25-600 °C. Optical microscopic photographs were obtained from a KEYENCE VHX-1000C super depth of field three-dimensional (3D) microscopy. Atom Absorption Spectroscopy (AAS) was performed on a TAS-990NFG atom absorption spectroscopy instrument. X-ray photoelectron spectrum (XPS) was carried out by Axis Ultra Imaging Photoelectron spectrometer (Kratos Analytical Ltd. Japan), from which can analyze the composition of elements. Variable-temperature magnetic susceptibility on polycrystalline samples was performed on a Quantum Design MPMS-XL-7 SQUID magnetometer over the temperature range 2-400 K at 1000 Oe. The molar susceptibility was corrected for diamagnetic contributions using Pascal's constants and the increment method. Samples (ca. 30 mg) were restrained with petroleum jelly to prevent decomposing of the crystallites. The room-temperature Mössbauer measurements were obtained on a constant-acceleration conventional spectrometer with a 25 mCi source of 57Co (Pd matrix). The isomer shift values (δ) are given with respect to metallic iron at room temperature. The absorber was a sample of microcrystalline powder of cages enclosed in a 20 mm diameter cylindrical plastic sample holder, the size of which had been determined to optimize the absorption. A least-squares computer program was used to fit the Mössbauer parameters and to determine their standard deviations of statistical origin.

2. Synthesis of 1, 8-di(imidazole-2-carboxaldehyde)octane

1.35 g (14 mmol) imidazole-2-carboxaldehyde, 1.36 g (5 mmol) 1,8-dibromooctane, 1.38 g (10 mmol) potassium carbonate and 25 mL DMF were added into a 50 mL flask in nitrogen atmosphere. The mixture was stirred for 3 days at 50 °C and cooling to room temperature. Then, the reaction mixture filtered to get yellow solution. With ethyl acetate (4×10 mL) extraction, the upper organic phase was collected. For collected liquid, washed with saturated aqueous solution of potassium chloride, and dried with anhydrous magnesium sulfate. Finally, the solvent was removed on a rotary evaporator to give 1.21 g of the desired product as yellow crystals (Yield: 80%). Pure light yellow crystals of 1,8-di(imidazole-2-carboxaldehyde)octane were obtained by recrystallizing the crude product from ethyl acetate. Elemental analysis (%) calcd for $C_{16}N_4H_{22}O_2$: C 63.55, N 18.53, H 7.33; found: C 63.62, N 18.46, H 7.45. IR (KBr, *v* cm^{-1}): 3109, 2931, 2856, 1723, 1684, 1474, 1410, 1335, 1305, 1157, 920, 771, 680. ^{1}H NMR (400 MHz, CD_3CN, δ ppm) 9.72 (s, $2H^1$), 7.36 (s, $2H^2$), 7.24 (s, $2H^3$), 4.37 (t, *J* = 6.4 Hz, $4H^4$), 1.75 (m, $4H^5$), 1.29 (m, $8H^{6,7}$). ^{13}C NMR (400 MHz, CD_3CN, δ ppm): 181.88, 131.13, 127.03, 117.29, 47.20, 30.59, 28.51, 25.87.

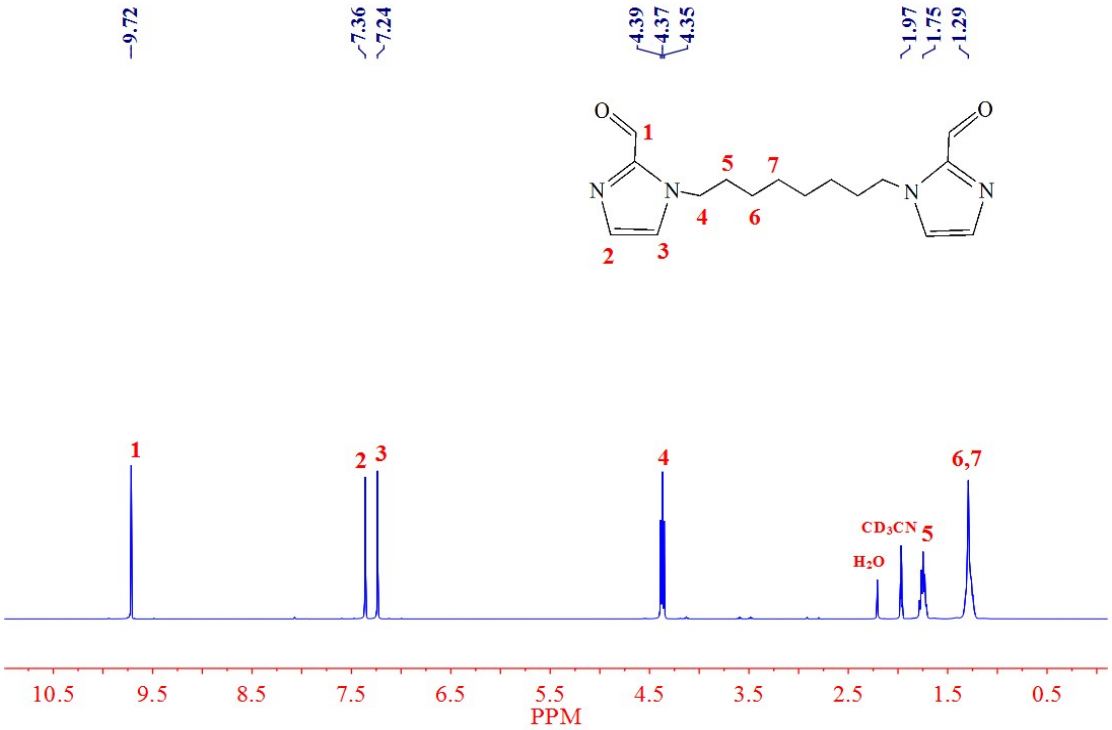

Figure. S1. ^{1}H NMR spectrum of 1, 8-di(imidazole-2-carboxaldehyde)octane.

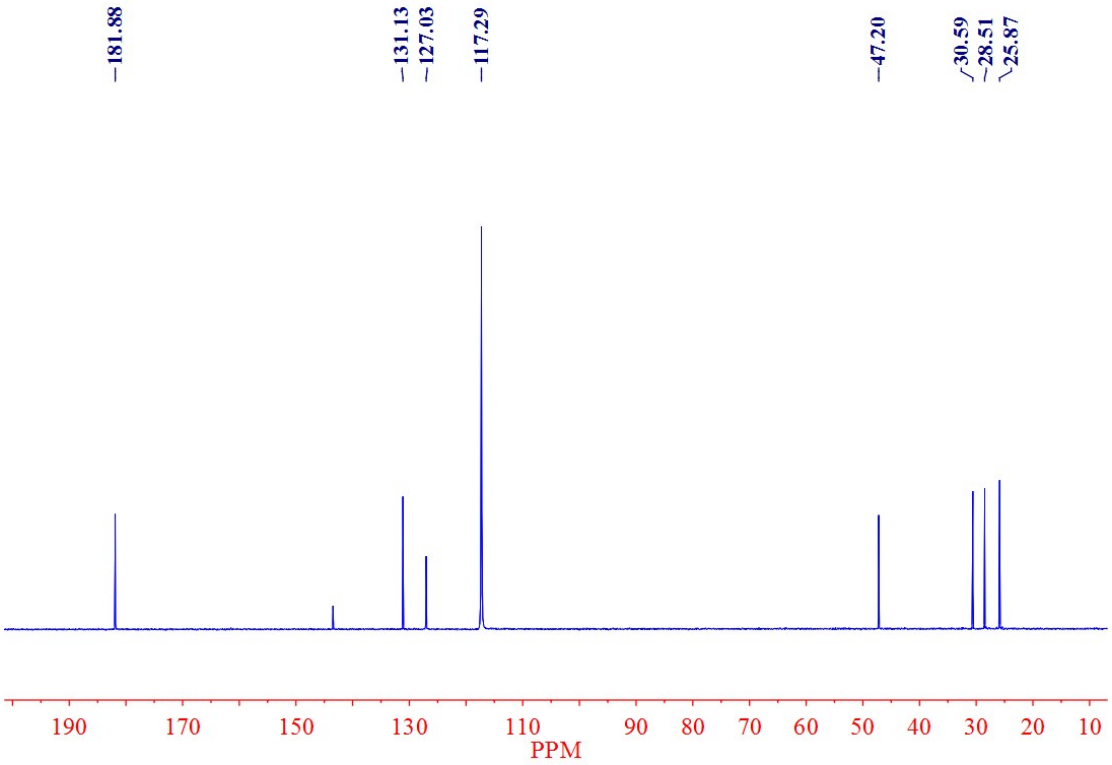

Figure. S2. ^{13}C NMR spectrum of 1, 8-di(imidazole-2-carboxaldehyde)octane.

3. Synthesis of cage 1

1,8-di(imidazole-2-carboxaldehyde)octane (60.5 mg, 0.2 mmol), (*R*)-1-phenylethylamine (48.9 mg, 0.4 mmol), and $Fe(BF_4)_2{\cdot}6H_2O$ (45.0 mg, 0.13 mmol) were added to a flask with 15 mL of acetonitrile in nitrogen atmosphere. The solution was stirred and heated at 80 °C for 2 h, and the resulting purple solution was cooled and filtered. Next, the filtrate was transferred to three separate test tubes (1.5 × 10 cm), and then the test tubes were placed in the jar (500 mL) containing 200 mL diethyl ether. Dark purple crystals of 111.1 mg were grown on the test tubes after 7 days through slow diffusion of diethyl ether into the filtrate at room temperature. Yield: 84%. Elemental analysis (%) calcd for $Fe_4C_{192}N_{36}H_{240}B_8F_{32}$: C 58.09, N 12.70, H 6.09; found: C 58.12, N 12.65, H 6.14. UV-vis λmax: 209, 285, 540 nm. IR (KBr, ν cm^{-1}): 3146, 2932, 2858, 1575, 1530, 1491, 1448, 1379, 1286, 1061, 918, 845, 762, 704, 629. ^{1}H NMR (400 MHz, CD_3CN, δ ppm): 11.83 (s, 2H^6), 9.34 (s, 2H^7), 7.91 (s, 2H^8), 7.19 (t, J =6.9 Hz, 2H^1), 7.03 (t, J = 6.5 Hz, 4H^2), 6.40 (d, J = 6.4 Hz, 4H^3), 3.95 (d, J = 13.7 Hz, 2H^4), 3.67 (t, J = 12.1 Hz, 4H^9), 2.17 (d, J = 6.5 Hz, 6H^5), 1.27 (m, 4H^{10}), 0.81 (m, 4H^{11}), 0.44 (m, 4H^{12}).

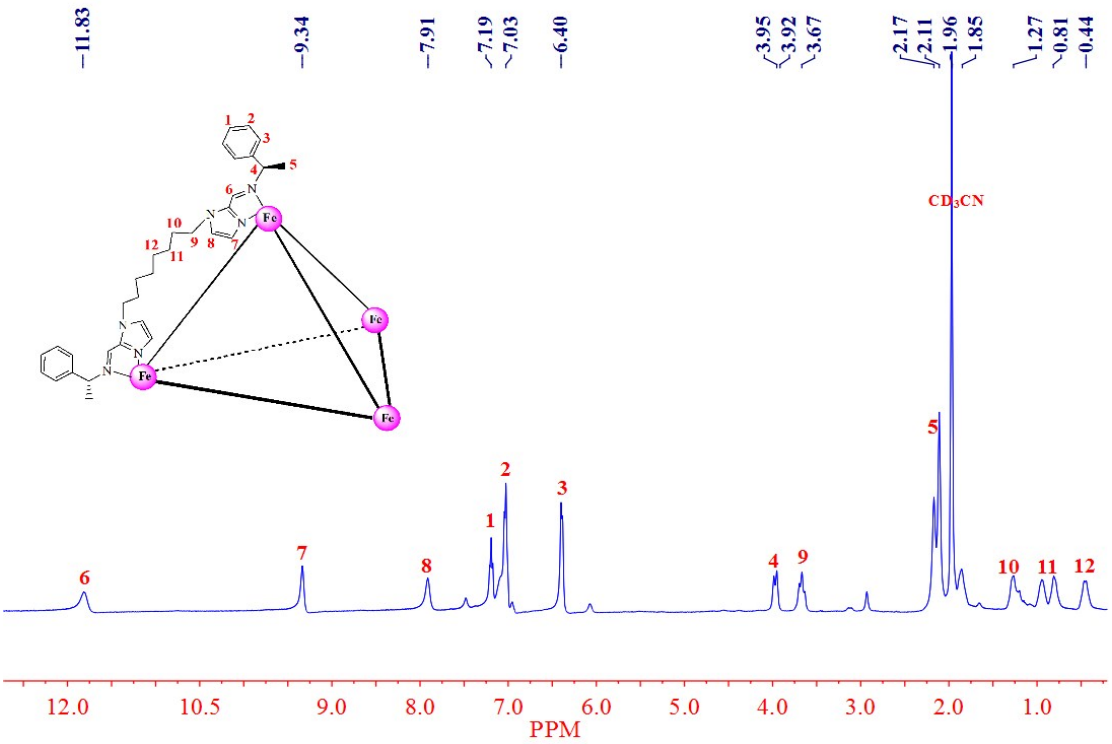

Figure. S3. ^{1}H NMR spectrum of cage **1**.

4. Synthesis of cage 2

This complex was prepared following a procedure similar to that for cage **1** except that $Ni(BF_4)_2 \cdot 6H_2O$ (45.4 mg, 0.13 mmol) instead of $Fe(BF_4)_2 \cdot 6H_2O$ was used. The colorless crystals of 103.5 mg were obtained after 7 days. Yield: 78%. Elemental analysis (%) calcd for $Ni_4C_{192}N_{36}H_{240}B_8F_{32}$: C 57.92, N 12.66, H 6.08; found: C 57.86, N 12.70, H 6.05. UV-vis λmax: 208, 302 nm. IR (KBr, ν cm^{-1}): 3123, 2932, 2858, 1618, 1494, 1445, 1384, 1308, 1062, 920, 842, 764, 706, 625.

5. X-ray crystal structures

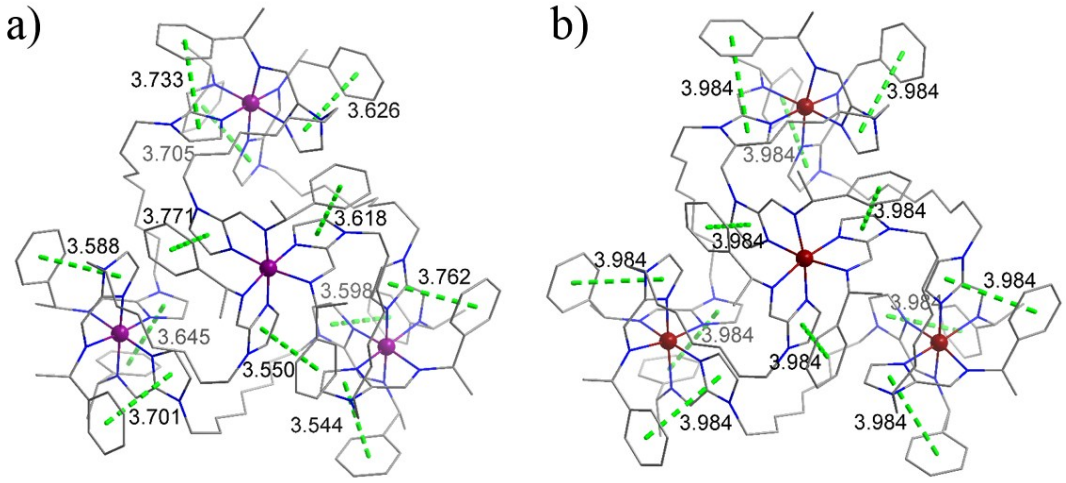

Figure. S4. Intramolecular π–π interactions (green dashed lines) of (a) **1**; (b) **2**. All H atoms and lattice tetrafluoroborate anions have been removed for clarity.

6. Recognition of I_2 and TCNQ

2-I_2: 1,8-di(imidazole-2-carboxaldehyde)octane (60.5 mg, 0.2 mmol), (*R*)-1-phenylethylamine (48.9 mg, 0.4 mmol), and $Ni(BF_4)_2{\cdot}6H_2O$ (45.4 mg, 0.13 mmol) were added to a flask with 15 mL of acetonitrile in nitrogen atmosphere. The solution was stirred and heated at 80 °C for 2 h, and the resulting light yellow solution was cooled and filtered. Next, the filtrate was transferred to three separate test tubes (1.5 × 10 cm), and then the test tubes were placed in the jar (500 mL) containing 200 mL diethyl ether. Colorless crystals of cage **2** were grown on the test tubes after 7 days through slow diffusion of diethyl ether into the filtrate at room temperature. Then the iodine diethyl ether solution (1 mL 100 mg/mL) was slowly added into one test tube. Dark purple crystals **2**-I_2 of 95.2 mg were harvested after 24 hours (yield of 92% based on **2**). UV-vis λmax: 206, 294, 360 nm. IR (KBr, ν cm^{-1}): 3123, 2932, 2858, 1618, 1494, 1445, 1384, 1308, 1062, 920, 842, 764, 706, 625.

2-TCNQ: single crystal **2**-TCNQ were prepared following a procedure similar to that for **2**-I_2 except that 7,7,8,8-tetracyanodimethanoquinone (TCNQ) acetonitrile solution (1 mL 100 mg/mL) instead of iodine diethyl ether solution was used. Dark green

crystals **2**-TCNQ of 96.3 mg were harvested after 24 hours (yield of 93% based on **2**). UV-vis λmax: 206, 300, 482 nm. IR (KBr, ν cm^{-1}): 3123, 2932, 2858, 2179, 2152, 1618, 1494, 1445, 1384, 1308, 1062, 920, 842, 824, 764, 706, 625.

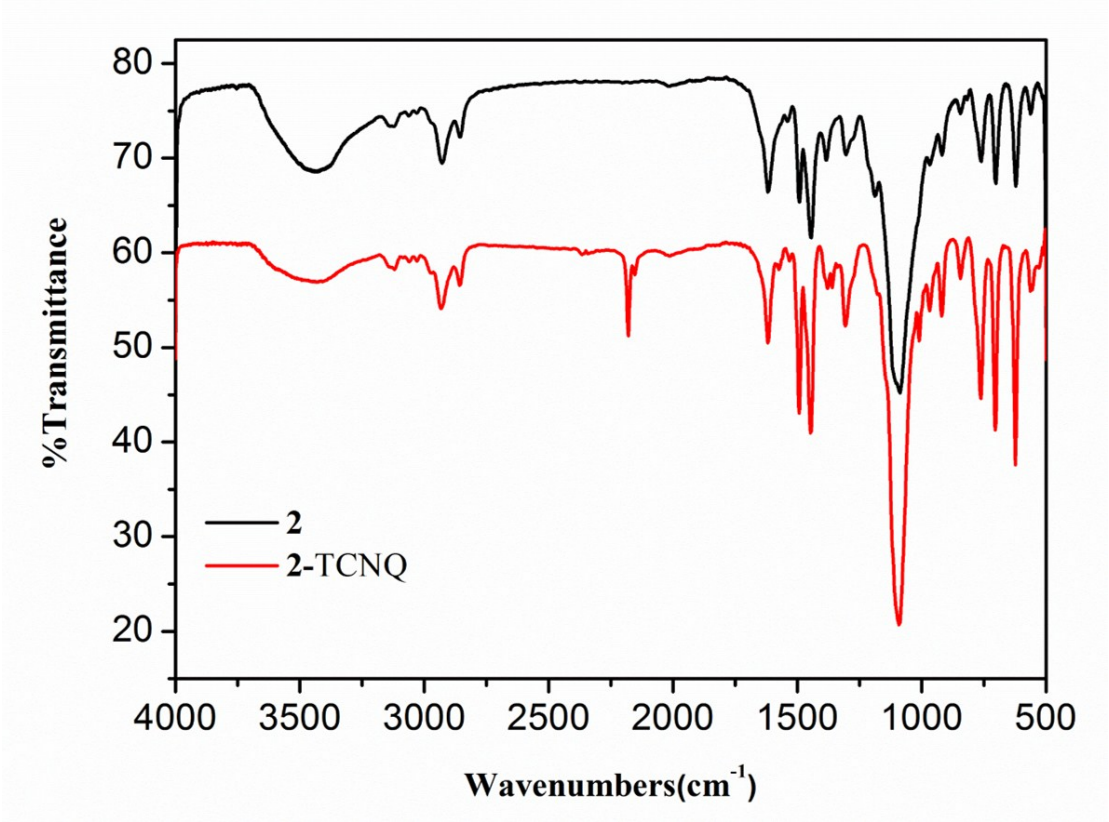

Figure. S5. IR spectra for cages **2** and **2**-TCNQ.

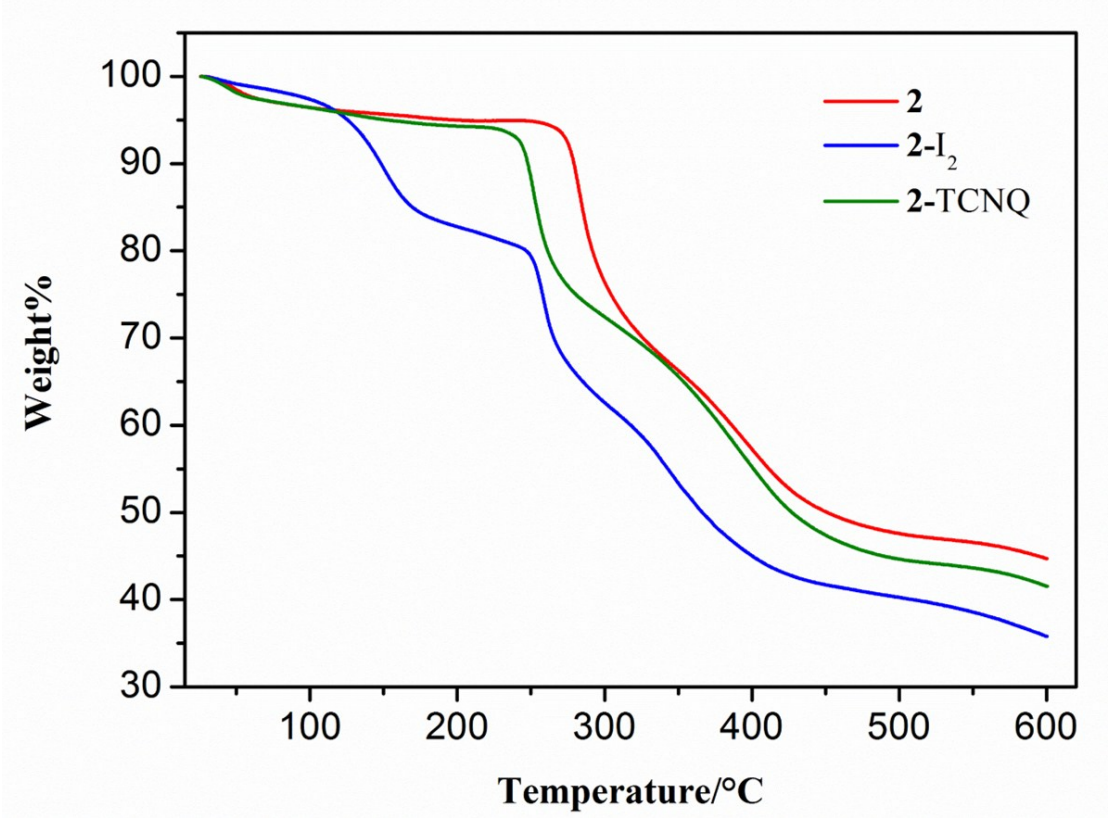

Figure. S6. Thermogravimetric analysis (TGA) for cages **2**, **2**-I_2 and **2**-TCNQ.

In **2**, **2**-I_2 and **2**-TCNQ, the first weigh loss until 263 °C, 102 °C and 235 °C was due to the volatile solvent molecules, respectively (obsd 5.42%, 2.75%, 6.48%). For **2**-I_2, the second weight loss at 100-250 °C because of the absorded 2.74 I_2 molecules (obsd 17.45%). For **2**-TCNQ, the second weight loss at 235-335 °C because of the absorded 5.06 TCNQ molecules (obsd 25.84%).The decomposition of the organic links in the anhydrous compounds occur at 263-600 °C, 248-600 °C, 335-600 °C, respectively.

7. Experiment of metal-center exchange

Generally: Single crystals **1** and **2** hardly retain their crystalline order after leaving mother liquid. SCSC metal-center exchange was unsuccessful when solvents (deionized water, dichloromethane, ethyl alcohol, cyclohexane etc.) were used. This result prompted us to study the possibility of SCSC metal-center exchange in mother liquid (Figure. S7). Different temperature (268-308 K) and the added $M(BF_4)_2$ concentration (10-200 mg/mL) were investigated to consider their influence on the selection. Preliminary results showed that metal-center exchange processes were

performed with higher temperature and $M(BF_4)_2$ concentration, the faster reaction rate becomes. The most suitable temperature (298 K) and $M(BF_4)_2$ concentration (100 mg/mL) were chosen to conduct the metal-center exchange processes. The transformation of single crystals **2** by Co^{2+}, Cu^{2+}, Zn^{2+}, Mn^{2+} were carry out through a similar procedure that for SCSC metal-center exchange of single crystals **2** in mother liquid. Soaking single crystals **2** in the $M(BF_4)_2$ (M= Co^{2+}, Cu^{2+}, Zn^{2+}, Mn^{2+}) solution for 1 week, the form and color of **2** unchanged, and no metal exchange phenomena were observed as confirmed by AAS analysis.

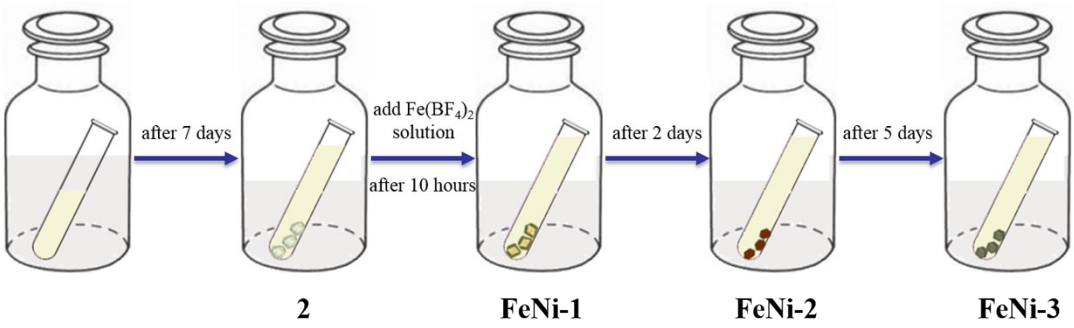

Figure. S7. SCSC metal-center exchange of single crystals **2** in mother liquid.

Synthesis of FeNi-1

1,8-di(imidazole-2-carboxaldehyde)octane (60.5 mg, 0.2 mmol), (*R*)-1-phenylethylamine (48.9 mg, 0.4 mmol), and $Ni(BF_4)_2{\cdot}6H_2O$ (45.4 mg, 0.13 mmol) were added to a flask with 15 mL of acetonitrile in nitrogen atmosphere. The solution was stirred and heated at 80 °C for 2 h, and the resulting light yellow solution was cooled and filtered. Next, the filtrate was transferred to three separate test tubes (1.5 × 10 cm), and then the test tubes were placed in the jar (500 mL) containing 200 mL diethyl ether. Colorless crystals of cage **2** were grown on the test tubes after 7 days through slow diffusion of diethyl ether into the filtrate at room temperature. Then the $Fe(BF_4)_2$ acetonitrile solution (1 mL 100 mg/mL) was slowly added into one test tube at ambient temperature under nitrogen atmosphere. Yellow crystals **FeNi-1** of 98.2 mg were harvested after 10 hours (yield of 95% based on **2**). Atomic absorption spectroscopy (AAS): Fe 19.82%, Ni 80.18%. Elemental analysis (%) calcd for $Ni_{3.20}Fe_{0.80}C_{192}N_{36}H_{240}B_8F_{32}$: C 57.95, N 12.67, H 6.08; found: C 57.98, N 12.65, H

6.04. UV-vis λmax: 208, 300 nm. IR (KBr, ν cm^{-1}): 3123, 2932, 2858, 1618, 1491, 1447, 1380, 1305, 1062, 922, 845, 764, 704, 625.

Synthesis of FeNi-2

Single crystals of **FeNi-2** were prepared in a similar way that for **FeNi-1**. Red crystals **FeNi-2** of 99.5 mg were harvested after 2 days (yield of 96% based on **2**). Atomic absorption spectroscopy (AAS): Fe 33.04%, Ni 66.96%. Elemental analysis (%) calcd for $Ni_{2.67}Fe_{1.33}C_{192}N_{36}H_{240}B_8F_{32}$: C 57.98, N 12.68, H 6.08; found: C 57.97, N 12.69, H 6.08. UV-vis λmax: 209, 299 nm. IR (KBr, ν cm^{-1}): 3123, 2928, 2854, 1618, 1445, 1383, 1304, 1067, 910, 845, 760, 702, 702, 621.

Synthesis of FeNi-3

Single crystals of **FeNi-3** were prepared in a similar way that for **FeNi-1**. Dark purple crystals **FeNi-3** of 96.9 mg were harvested after 5 days (yield of 94% based on **2**). Atomic absorption spectroscopy (AAS): Fe 51.54%, Ni 48.46%. Elemental analysis (%) calcd for $Ni_{2.00}Fe_{2.00}C_{192}N_{36}H_{240}B_8F_{32}$: C 58.00, N 12.68, H 6.08; found: C 58.02, N 12.65, H 6.09. UV-vis λmax: 209, 298, 540 nm. IR (KBr, ν cm^{-1}): 3123, 2932, 2858, 1618, 1575, 1491, 1447, 1383, 1306, 1062, 918, 845, 764, 704, 623.

Competitive crystallization reactions

Competitive crystallization reactions were carried out through subcomponent self-assembly of $Fe(BF_4)_2{\cdot}6H_2O$, $Ni(BF_4)_2{\cdot}6H_2O$, 1,8-di(imidazole-2-carboxaldehyde)octane, and (*R*)-1-phenylethylamine in 1:1:3:6 molar ratio. Dark purple dodecahedral crystals like cage **FeNi-3** (Fig. 3e) were grown on the test tubes after 7 days through slow diffusion of diethyl ether into the filtrate at room temperature. Fe/Ni ratio is approximately assigned as 1/1, which was investigated by AAS analysis.

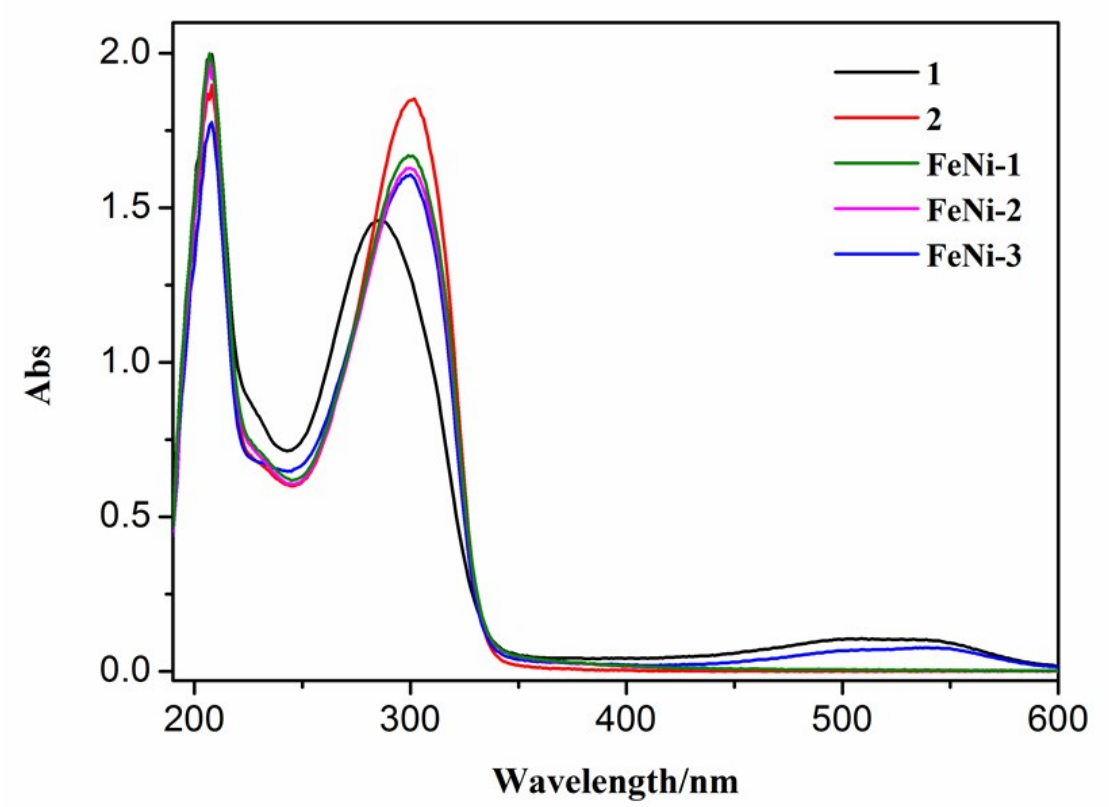

Figure. S8. UV-vis spectra of cages **1**, **2**, **FeNi-1**, **FeNi-2**, and **FeNi-3** in CH_3CN (10^{-5} mol·L^{-1}).

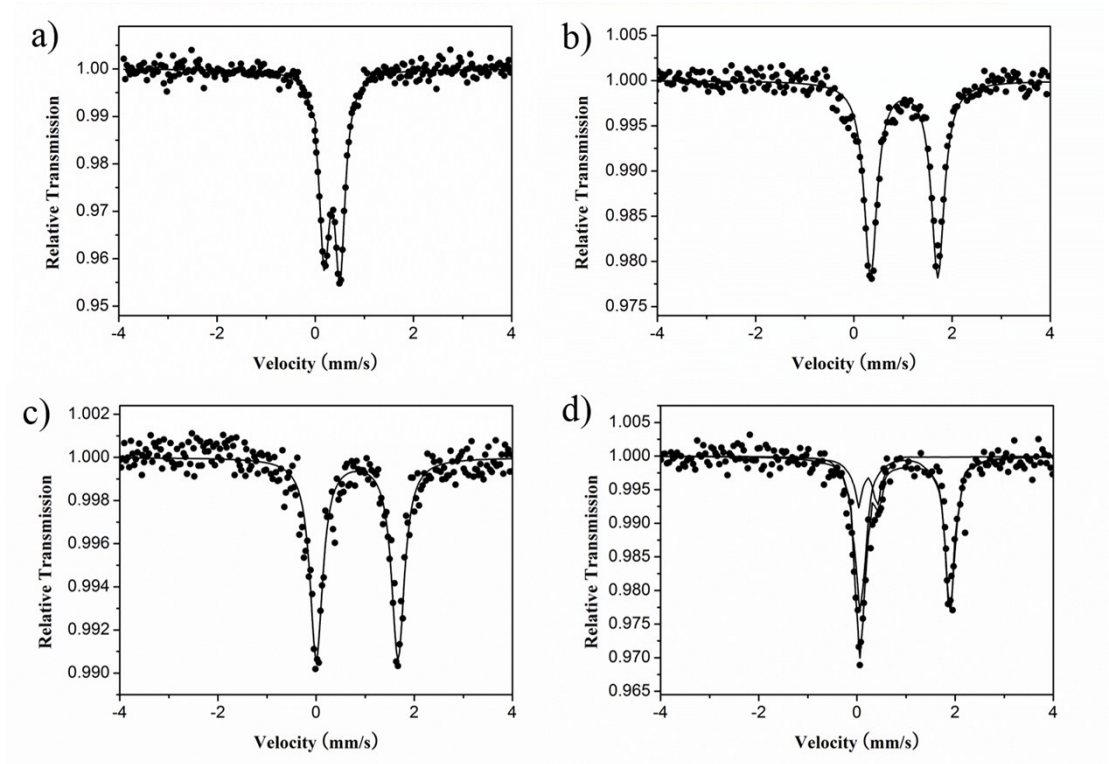

Figure. S9. ^{57}Fe Mössbauer spectra of (a) **1**, (b) **FeNi-1**, (c) **FeNi-2**, and (d) **FeNi-3** at 295K.

Table S1 Mössbauer parameters for cages **1**, **FeNi-1**, **FeNi-2**, and **FeNi-3**.

	T(K)	δ(mm·s^{-1})	ΔE_Q(mm·s^{-1})	Γ(mm·s^{-1})	A_{HS}/A_{tot}(%)
1	295	0.34(1)	0.32(2)	0.25(0)	0
FeNi-1	295	1.02(4)	1.37(0)	0.31(7)	100
FeNi-2	295	0.84(2)	1.66(2)	0.32(2)	100
FeNi-3	295	1.06(1)	1.68(2)	0.34(2)	86.8
		0.41(1)	0.38(4)	0.41(2)	

δ, isomer shift; ΔE_Q, quadrupole-split splitting; Γ, half-height width; A/A_{tot}, area ratio.

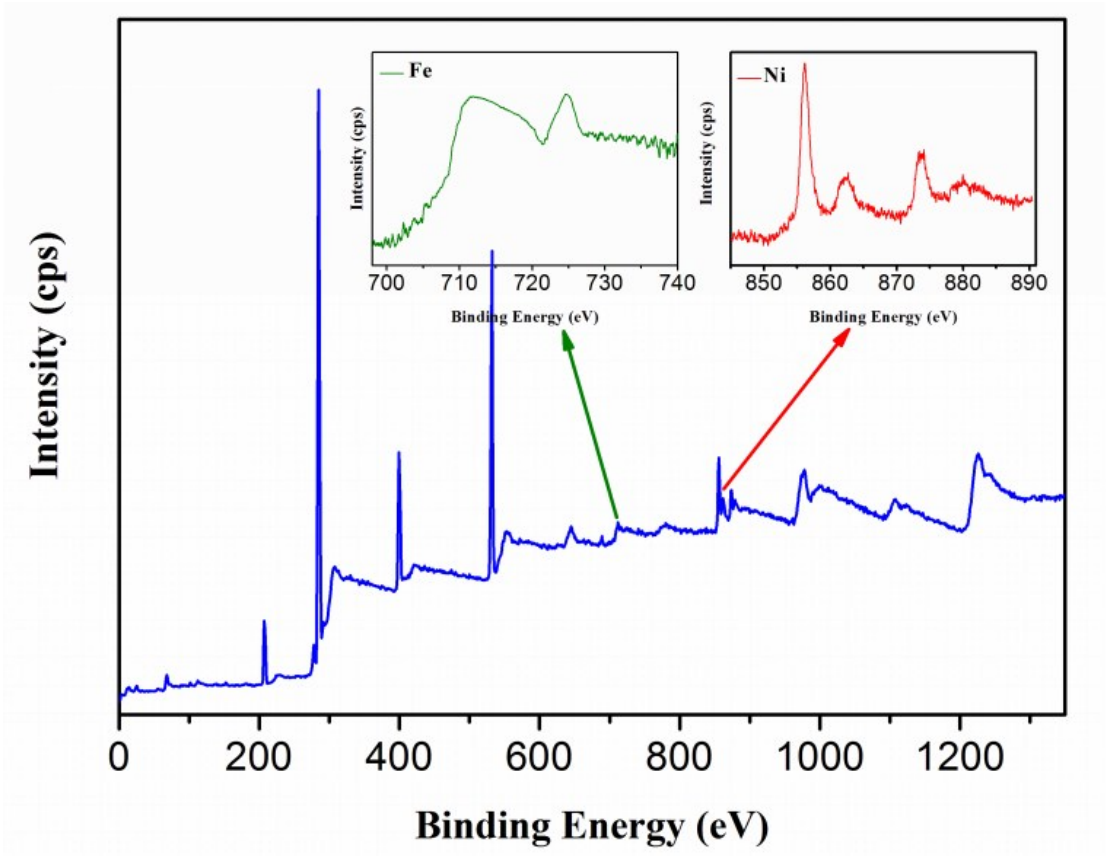

Figure. S10. XPS spectrum of **FeNi-1** and high resolution spectrum for Fe 2p and Ni 2p in **FeNi-1**, respectively.

8. X-ray Crystallography

The crystal structures were determined on a Siemens (Bruker) SMART CCD diffractometer using monochromated Mo $K\alpha$ radiation (λ = 0.71073 Å) at 173 K. Cell parameters were retrieved using SMART software and refined using SAINT[1] on all observed reflections. The highly redundant data sets were reduced using SAINT[1] and corrected for Lorentz and polarization effects. Absorption corrections were applied using SADABS[2] supplied by Bruker. Structures were solved by direct methods using the program SHELXL-97.[3] All of the non-hydrogen atoms except the disordered solvent molecules and anions were refined with anisotropic thermal displacement coefficients. Hydrogen atoms of organic ligands were located geometrically and refined in a riding model, whereas those of solvent molecules were not treated during the structural refinements. Disorder was modelled using standard crystallographic methods including constraints, restraints and rigid bodies where necessary. For cage **2** and **FeNi-1**, twelve phenylethylamine groups (C5-C12) are disordered. The crystals of **1**, **2** and **FeNi-1** decayed rapidly out of solvent. Despite rapid handling and long exposure times, the data collected are less than ideal quality. Nevertheless, the data for **1**, **2** and **FeNi-1** are of more than sufficient quality to unambiguously establish the connectivity of the structures. Reflecting the instability of the crystals, there is a large area of smeared electron density present in the lattice. Despite many attempts to model this region of disorder as a combination of solvent molecules and partial anions no reasonable fit could be found and accordingly this region was treated with the SQUEEZE function of PLATON. Final crystallographic data and values of R_1 and wR for **1**, **2** and **FeNi-1** are listed in Table S2. Selected bond distances and angles are given in Table S3.

Table S2 Summary of crystallographic data for cages **1**, **2** and **FeNi-1**.

	1	**2**	**FeNi-1**
formula	$C_{192}H_{240}B_{6.25}F_{25}Fe_4N_{36}$	$C_{192}H_{240}B_4F_{16}N_{36}Ni_4$	$C_{192}H_{240}B_4F_{16}Fe_{0.80}N_{36}Ni_{3.20}$
fw	3818.11	3631.85	3631.93
T (K)	173(2)	173(2)	173(2)
λ (Å)	0.71073	0.71073	0.71073
crystal system	Hexagonal	Cubic	Cubic
space group	$P6_3$	$I23$	$I23$
a (Å)	40.6845(16)	23.2474(7)	23.2506(7)
b (Å)	40.6845(16)	23.2474(7)	23.2506(7)
c (Å)	34.133(3)	23.2474(7)	23.2506(7)
α (^{0})	90	90	90
β (^{0})	90	90	90
γ (^{0})	120	90	90
V (Å^3)	48928(6)	12563.9(7)	12569.1(7)
Z	2	2	2
D_{calc} (Mg/m^3)	1.037	1.052	1.051
μ (mm^{-1})	0.3	0.367	0.353
F(000)	16034	4168	4165
θ (^{0})	0.83-23.33	3.28-25.34	3.28-25.34
index ranges	□31<=h<=31 □25<=k<=44 □36<=l<=22	□7<=h<=25 □23<=k<=28 □22<=l<=27	□26<=h<=23 □7<=k<=25 □27<=l<=23
reflections collected	61363	5945	7282
GOF (F^2)	1.061	1.015	1.198
R_1[a],wR_2[b](I>2σ(I))	0.1209, 0.3020	0.0702, 0.1609	0.0912, 0.2277
R_1[a],wR_2[b](all data)	0.1977, 0.3466	0.1197, 0.1812	0.1429, 0.2470

$R_1{}^a = \Sigma||F_o| - |F_c||/\Sigma|F_o|$. $wR_2{}^b = [\Sigma w(F_o{}^2 - F_c{}^2)^2/\Sigma w(F_o{}^2)]^{1/2}$

Table S3. Selected bond lengths [Å] and angles [°] for cages **1**, **2** and **FeNi-1**.

1			
N(1A)-Fe(1)	1.931(9)	N(1H)-Fe(4)	1.925(13)
N(3A)-Fe(1)	1.965(10)	N(3H)-Fe(4)	1.893(17)
N(1F)-Fe(1)	1.947(10)	N(1J)-Fe(4)	1.885(16)
N(3F)-Fe(1)	2.033(11)	N(3J)-Fe(4)	1.974(13)
N(1I)-Fe(1)	1.940(11)	N(1L)-Fe(4)	1.950(12)
N(3I)-Fe(1)	1.979(9)	N(3L)-Fe(4)	2.013(13)
N(1D)-Fe(2)	1.917(10)	N(1M)-Fe(5)	1.921(14)
N(3D)-Fe(2)	2.008(10)	N(3M)-Fe(5)	2.059(13)
N(1E)-Fe(2)	1.973(10)	Fe(5)-N(1M)#1	1.921(14)
N(3E)-Fe(2)	2.052(10)	Fe(5)-N(1M)#2	1.921(14)
N(1K)-Fe(2)	1.943(10)	Fe(5)-N(3M)#1	2.059(14)
N(3K)-Fe(2)	2.042(12)	Fe(5)-N(3M)#2	2.059(13)
N(1G)-Fe(3)	1.961(12)	N(1N)-Fe(6)	1.955(12)
N(3G)-Fe(3)	2.040(11)	N(3N)-Fe(6)	1.962(12)
N(1B)-Fe(3)	1.932(10)	Fe(6)-N(1P)#2	1.904(12)
N(3B)-Fe(3)	2.047(11)	Fe(6)-N(3P)#2	2.039(12)
N(1C)-Fe(3)	1.952(10)	N(1Q)-Fe(6)	2.003(12)
N(3C)-Fe(3)	2.028(11)	N(3Q)-Fe(6)	1.988(12)
N(1A)-Fe(1)-N(1I)	92.7(5)	N(1J)-Fe(4)-N(3H)	174.6(7)
N(1A)-Fe(1)-N(1F)	91.0(4)	N(1J)-Fe(4)-N(1H)	89.5(6)
N(1I)-Fe(1)-N(1F)	89.2(4)	N(3H)-Fe(4)-N(1H)	85.3(7)
N(1A)-Fe(1)-N(3A)	83.7(4)	N(1J)-Fe(4)-N(1L)	88.5(7)
N(1I)-Fe(1)-N(3A)	93.7(5)	N(3H)-Fe(4)-N(1L)	93.1(7)
N(1F)-Fe(1)-N(3A)	174.1(4)	N(1H)-Fe(4)-N(1L)	92.8(5)
N(1A)-Fe(1)-N(3I)	175.4(5)	N(1J)-Fe(4)-N(3J)	84.5(6)
N(1I)-Fe(1)-N(3I)	82.7(4)	N(3H)-Fe(4)-N(3J)	94.1(6)
N(1F)-Fe(1)-N(3I)	90.0(4)	N(1H)-Fe(4)-N(3J)	90.2(6)
N(3A)-Fe(1)-N(3I)	95.5(4)	N(1L)-Fe(4)-N(3J)	172.3(7)
N(1A)-Fe(1)-N(3F)	91.0(4)	N(1J)-Fe(4)-N(3L)	93.5(7)
N(1I)-Fe(1)-N(3F)	171.7(4)	N(3H)-Fe(4)-N(3L)	91.9(7)
N(1F)-Fe(1)-N(3F)	83.3(5)	N(1H)-Fe(4)-N(3L)	173.4(6)
N(3A)-Fe(1)-N(3F)	94.1(5)	N(1L)-Fe(4)-N(3L)	81.3(5)
N(3I)-Fe(1)-N(3F)	93.6(4)	N(3J)-Fe(4)-N(3L)	96.0(6)
N(1D)-Fe(2)-N(1K)	90.5(4)	N(1M)#1-Fe(5)-N(1M)	91.3(6)
N(1D)-Fe(2)-N(1E)	94.0(5)	N(1M)#1-Fe(5)-N(1M)#2	91.3(6)
N(1K)-Fe(2)-N(1E)	92.0(4)	N(1M)-Fe(5)-N(1M)#2	91.3(6)
N(1D)-Fe(2)-N(3D)	83.7(4)	N(1M)#1-Fe(5)-N(3M)#1	81.4(6)
N(1K)-Fe(2)-N(3D)	173.5(4)	N(1M)-Fe(5)-N(3M)#1	171.2(5)

N(1E)-Fe(2)-N(3D)	91.5(4)	N(1M)#2-Fe(5)-N(3M)#1	93.8(5)
N(1D)-Fe(2)-N(3K)	90.1(5)	N(1M)#1-Fe(5)-N(3M)#2	171.2(5)
N(1K)-Fe(2)-N(3K)	82.0(5)	N(1M)-Fe(5)-N(3M)#2	93.8(5)
N(1E)-Fe(2)-N(3K)	172.8(4)	N(1M)#2-Fe(5)-N(3M)#2	81.4(6)
N(3D)-Fe(2)-N(3K)	94.8(5)	N(3M)#1-Fe(5)-N(3M)#2	94.0(6)
N(1D)-Fe(2)-N(3E)	175.0(4)	N(1M)#1-Fe(5)-N(3M)	93.8(5)
N(1K)-Fe(2)-N(3E)	92.4(4)	N(1M)-Fe(5)-N(3M)	81.4(6)
N(1E)-Fe(2)-N(3E)	81.9(4)	N(1M)#2-Fe(5)-N(3M)	171.2(5)
N(3D)-Fe(2)-N(3E)	93.5(4)	N(3M)#1-Fe(5)-N(3M)	94.0(6)
N(3K)-Fe(2)-N(3E)	94.3(5)	N(3M)#2-Fe(5)-N(3M)	94.0(6)
N(1B)-Fe(3)-N(1C)	92.3(4)	N(1P)#2-Fe(6)-N(1N)	91.0(5)
N(1B)-Fe(3)-N(1G)	94.1(4)	N(1P)#2-Fe(6)-N(3N)	92.0(5)
N(1C)-Fe(3)-N(1G)	94.2(5)	N(1N)-Fe(6)-N(3N)	82.3(5)
N(1B)-Fe(3)-N(3C)	173.0(4)	N(1P)#2-Fe(6)-N(3Q)	172.4(5)
N(1C)-Fe(3)-N(3C)	82.2(4)	N(1N)-Fe(6)-N(3Q)	91.2(5)
N(1G)-Fe(3)-N(3C)	90.7(4)	N(3N)-Fe(6)-N(3Q)	95.5(5)
N(1B)-Fe(3)-N(3G)	92.5(4)	N(1P)#2-Fe(6)-N(1Q)	91.4(5)
N(1C)-Fe(3)-N(3G)	173.5(4)	N(1N)-Fe(6)-N(1Q)	94.3(5)
N(1G)-Fe(3)-N(3G)	81.0(5)	N(3N)-Fe(6)-N(1Q)	175.2(5)
N(3C)-Fe(3)-N(3G)	93.3(4)	N(3Q)-Fe(6)-N(1Q)	81.2(5)
N(1B)-Fe(3)-N(3B)	82.9(4)	N(1P)#2-Fe(6)-N(3P)#2	83.4(5)
N(1C)-Fe(3)-N(3B)	90.0(4)	N(1N)-Fe(6)-N(3P)#2	173.8(5)
N(1G)-Fe(3)-N(3B)	174.9(5)	N(3N)-Fe(6)-N(3P)#2	95.1(5)
N(3C)-Fe(3)-N(3B)	92.8(5)	N(3Q)-Fe(6)-N(3P)#2	94.6(5)
N(3G)-Fe(3)-N(3B)	95.0(4)	N(1Q)-Fe(6)-N(3P)#2	88.7(5)
		2	
N(1)-Ni(1)	2.063(4)	N(3)-Ni(1)	2.154(4)
Ni(1)-N(1)#1	2.063(4)	Ni(1)-N(3)#2	2.154(4)
Ni(1)-N(1)#2	2.063(4)	Ni(1)-N(3)#1	2.154(4)
N(1)-Ni(1)-N(1)#1	92.78(18)	N(1)-Ni(1)-N(3)#1	91.76(18)
N(1)-Ni(1)-N(1)#2	92.78(18)	N(3)#2-Ni(1)-N(3)#1	96.71(16)
N(1)#1-Ni(1)-N(1)#2	92.78(18)	N(3)#2-Ni(1)-N(3)	96.71(16)
N(1)#2-Ni(1)-N(3)#2	79.24(18)	N(3)#1-Ni(1)-N(3)	96.71(16)
N(1)-Ni(1)-N(3)	79.24(18)	N(1)-Ni(1)-N(3)#2	171.01(19)
N(1)#1-Ni(1)-N(3)#1	79.24(18)	N(1)#2-Ni(1)-N(3)#1	171.00(19)
N(1)#1-Ni(1)-N(3)#2	91.77(18)	N(1)#1-Ni(1)-N(3)	171.00(19)
N(1)#2-Ni(1)-N(3)	91.77(18)		
		FeNi-1	
N(1)-Ni(1)	2.072(6)	N(3)-Ni(1)	2.139(6)
Ni(1)-N(1)#1	2.072(6)	Ni(1)-N(3)#1	2.139(6)

Ni(1)-N(1)#2	2.072(6)	Ni(1)-N(3)#2	2.139(6)
N(1)#1-Ni(1)-N(3)#1	79.1(3)	N(1)-Ni(1)-N(1)#2	93.6(2)
N(1)-Ni(1)-N(3)	79.1(3)	N(3)#1-Ni(1)-N(3)	96.4(2)
N(1)#2-Ni(1)-N(3)#2	79.1(3)	N(3)#1-Ni(1)-N(3)#2	96.4(2)
N(1)#2-Ni(1)-N(3)	91.4(2)	N(3)-Ni(1)-N(3)#2	96.4(2)
N(1)#1-Ni(1)-N(3)#2	91.4(2)	N(1)#2-Ni(1)-N(3)#1	171.5(3)
N(1)-Ni(1)-N(3)#1	91.4(2)	N(1)#1-Ni(1)-N(3)	171.5(3)
N(1)#1-Ni(1)-N(1)	93.6(2)	N(1)-Ni(1)-N(3)#2	171.5(3)
N(1)#1-Ni(1)-N(1)#2	93.6(2)		

For **1**: #1 -x+y,-x+1,z #2 -y+1,x-y+1,z

For **2**: #1 -y+1,z,-x+1 #2 -z+1,-x+1,y #3 -x+2,-y,z

For **3**: #1 -y+1,z,-x+1 #2 -z+1,-x+1,y #3 -x+2,-y,z

9. References

[1] *SAINT-Plus*, version 6.02; Bruker Analytical X-ray System: Madison, WI, 1999.

[2] G. M. Sheldrick, *SADABS An empirical absorption correction program*; Bruker Analytical X-ray Systems: Madison, WI, 1996.

[3] G. M. Sheldrick, *SHELXTL-97*; Universität of Göttingen: Göttingen, Germany, 1997.